Journal of Ceramic Processing Research. Vol. 17, No. 4, pp. 295~299 (2016)

J O U R N A L O F
Ceramic Processing Research

Properties and rapid sintering of nanostructured WC and WC-TiAl hard materials by the pulsed current activated heating

Ga-Na Jung[a], Byung-Su Kim[b], Jin-Kook Yoon[c] and In-Jin Shon[a,*]

[a]*Division of Advanced Materials Engineering and the Research Center of Advanced Materials Development, Engineering College, Chonbuk National University, Chonbuk 561-756, Korea*

[b]*Minerals Resources Research Division, Korea Institute of Geoscience and Mineral Resources, Daejeon, 305-350 Korea*

[c]*Materials Architecturing Research Center, Korea Institute of Science and Technology, P.O. Box 131, Cheongryang, Seoul 130-650, Korea*

In the case of cemented WC, Ni or Co is added as a binder for the formation of composite structures. However, the high cost of Ni or Co, the low hardness and the low corrosion resistance of the WC-Ni and WC-Co cermets have generated interest in recent years for alternative binder phases. In this study, TiAl was used as a novel binder and consolidated by the pulsed current activated sintering (PCAS) method. Highly dense WC-TiAl with a relative density of up to 99% was obtained within 2 min by PCAS under a pressure of 80 MPa. The method was found to enable not only the rapid densification but also the inhibition of grain growth preserving the nano-scale microstructure. The addition of TiAl to WC enhanced the toughness without great decrease of hardness due to crack deflection and decrease of grain size.

Key words: Nanomaterials, Sintering, Hardness, Fracture Toughness, Hard Materials.

Introduction

The attractive properties of tungsten carbides is their high melting point (a peritectic melting temperature of 2785 ºC), high hardness (2854 kg/mm^2), high thermal and electrical conductivities, and relatively high chemical stability [1, 2]. Tungsten carbides are primarily used as cutting tools and abrasive materials in the form of composites with a binder metal, such as Co or Ni. However, these binder phases have inferior chemical characteristics compared to the carbide phase. Most notably, corrosion and oxidation occur preferentially in the binder phase [3]. Hence, the high cost of Ni or Co and the low corrosion resistance of the WC-Ni or WC-Co cermet have generated interest in recent years to find alternative binder phases [4, 5]. It has been reported that aluminides show a higher oxidation resistance, a higher hardness and a cheaper materials compared to Ni or Co [6].

The improvement of mechanical properties and stability of cemented carbides could be achieved through microstructural changes such as grain size refinement. Nanocrystalline materials have received much attention as advanced engineering materials with improved physical and mechanical properties [7, 8]. Since they possess a high strength and hardness as well as excellent ductility and toughness, they have garnered more attention recently [9, 10]. Recently, nanocrystalline powders have been produced by high-energy milling [11, 12]. The sintering temperature of high-energy mechanically milled powder is lower than that of unmilled powder due to the increased reactivity, internal and surface energies, and surface area of the milled powder, which contribute to its so-called mechanical activation [13-15]. However, the use of conventional methods to consolidate nanopowders often leads to grain growth due to the extended time for sintering. Generally, the grain growth could be minimized by sintering at lower temperatures and for shorter times. In this regard, the pulsed current activated sintering (PCAS) technique has been shown to be effective in the sintering of nanostructured materials in a very short time [16-19].

We present here the results of the sintering of WC and WC-TiAl composites by pulsed current activated sintering with simultaneous application of pulsed current and high-pressure. The goal of this study was to produce dense and nanocrystalline WC and WC-TiAl hard materials in very short sintering times (< 2 min). The effect of novel TiAl binder on the mechanical properties, and microstructure of WC-TiAl composites was also examined.

Experimental Procedures

The WC powder used in this study was supplied by Taegu Tec company (Korea). The average particle size was about 0.5 μm and the purity was 99.8%. TiAl (-100 mesh, 99% pure, Sejong Co.) was used as binder material. Powders of three compositions corresponding

*Corresponding author:
Tel : +82 63 270 2381
Fax: +82 63 270 2386
E-mail: ijshon@chonbuk.ac.kr

to WC, WC-5 vol.%TiAl, and WC-10 vol.%TiAl were prepared by weighting and milled in a high-energy ball mill (Pulverisette-5 planetary mill) at 250 rpm for 10 h. WC balls (9 mm in diameter) were used in a sealed cylindrical stainless steel vial under an argon atmosphere. The weight ratio of balls-to-powder was 30 : 1. The grain size of the powders was calculated from the full width at half-maximum (FWHM) of the diffraction peak by Suryanarayana and Grant Norton's formula [20].

$$B_r\ (B_{crystalline} + B_{strain})\ \cos\theta = k\ \lambda / L + \eta \sin\theta \qquad (1)$$

where B_r is the full width at half-maximum (FWHM) of the diffraction peak after instrumental correction; $B_{crystalline}$ and B_{strain} are FWHM caused by small grain size and internal stress, respectively; k is constant (with a value of 0.9); λ is wavelength of the X-ray radiation; L and η are grain size and internal strain, respectively; and θ is the Bragg angle. The parameters B and B_r follow Cauchy's form with the relationship: $B = B_r + B_s$, where B and B_s are the FWHM of the broadened Bragg peaks and the standard sample's Bragg peaks, respectively.

The milled powders were placed in a graphite die (outside diameter, 35 mm; inside diameter, 10 mm; height, 40 mm) and then introduced into the pulsed current activated sintering (PCAS) system made by Eltek Co. in the Republic of Korea. A schematic diagram of this system is shown in Ref. [16-19]. The PCAS apparatus includes a 30 kW power supply and a uniaxial press with a maximum load of 50 kN. The system was first evacuated and a uniaxial pressure of 80 MPa was applied. A pulsed current (on time; 20 μs, off time; 10 μs) was then activated and maintained until the densification rate became negligible, as indicated by the observed shrinkage of the sample. Sample shrinkage was measured in real time by a linear gauge measuring the vertical displacement. Temperature was measured by a pyrometer focused on the surface of the graphite die. A temperature gradient from the surface to the center of the sample is dependent on the heating rate, the electrical and thermal conductivities of the compact, and its relative density. The heating rates were approximately 1000 ^{o}K minute^{-1} during the process. At the end of the process, the current was turned off and the sample was allowed to cool to room temperature. The entire process of densification using the PCAS technique consists of four major control stages: chamber evacuation, pressure application, power application, and cooling off. The process was carried out under a vacuum of 5.33 Pa.

The relative densities of the sintered samples were measured by the Archimedes method. Microstructural information was obtained from the fracture surfaces. Compositional and microstructural analyses of the samples were carried out through X-ray diffraction (XRD), and field-emission scanning electron microscopy (FE-SEM). Vickers hardness was measured by performing indentations at a load of 20 kg_f with a dwell time of 15 s.

Results and Discussion

Fig. 1 shows FE-SEM images of raw materials. WC has round shape with very fine powder and TiAl has irregular shape with large particle size. X-ray diffraction patterns of raw powders were show in Fig. 2. Only WC peaks are detected in WC powder and only TiAl peaks are detected in TiAl powder. Fig. 3. Shows FE-SEM images of WC, WC-5 vol.% TiAl, and WC-10vol.% TiAl powders milled for 10h are shown in Fig. 3. The powders are very fine and have a round shape. X-ray diffraction patterns of the WC, WC-5 vol.% TiAl, and WC-10 vol.% TiAl powders after milling for 10 h are shown in Fig. 4. The broadening of WC peaks due to crystallite refinement and strain is evident after milling for 10 h. The milling process is known to introduce impurities from the ball and/or container. However, in this study, peaks other than WC were not identified. Particl size of WC was calculated from the plot of $B_r\ (B_{crystalline} + B_{strain})\ \cos\theta$ versus $\sin\theta$ in Suryanarayana and Grant Norton's formula [20]. The average grain sizes of the WC in the WC, WC-5 vol.% TiAl, and WC-10 vol.% TiAl powders after milling for 10 h calculated from the XRD data were

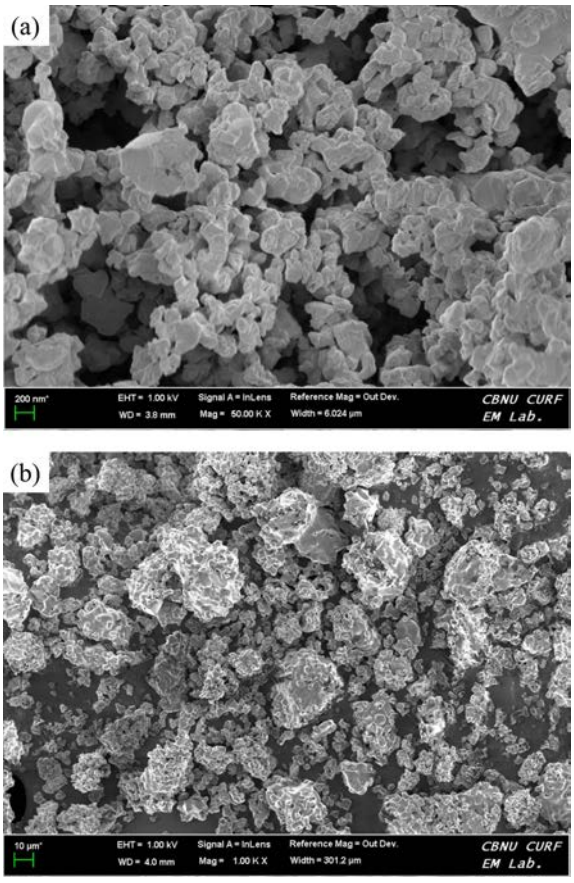

Fig. 1. FE-SEM images of raw materials : (a) WC, and (b) TiAl.

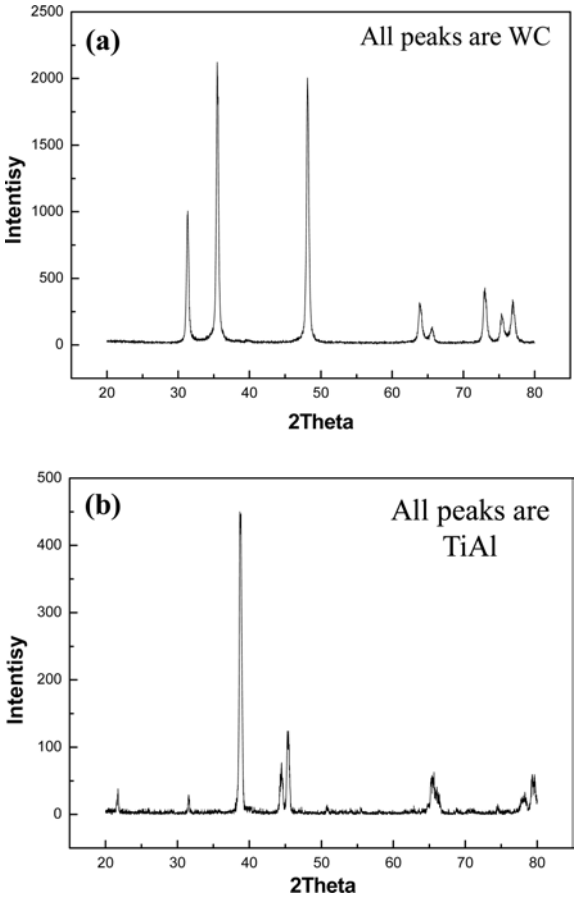

Fig. 2. XRD patterns of raw materials: (a) WC, and (b) TiAl.

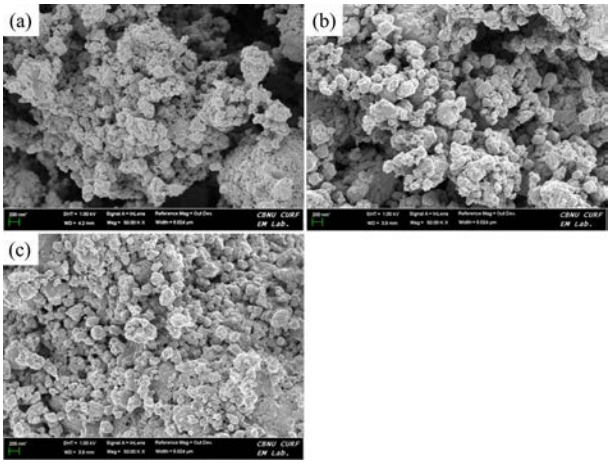

Fig. 3. FE-SEM images of powders milled for 10 h: (a) WC, (b) WC-5 vol.%TiAl, and (c) WC-10vol.%TiAl.

about 30, 17 and 16 nm, respectively.

Fig. 5 shows the XRD patterns of WC, WC-5 vol.% TiAl, and WC-10 vol.% TiAl sintered at 1600 ºC. In all cases, only WC peaks are detected. The average grain sizes of the WC calculated from the XRD data using Suryanarayana and Grant Norton's formula are about 70, 66, and 50 nm for the samples with WC, WC-5 vol.% TiAl, and WC-10 vol.% TiAl. FE-SEM images of the fracture surface after being sintered up to 1600ºC

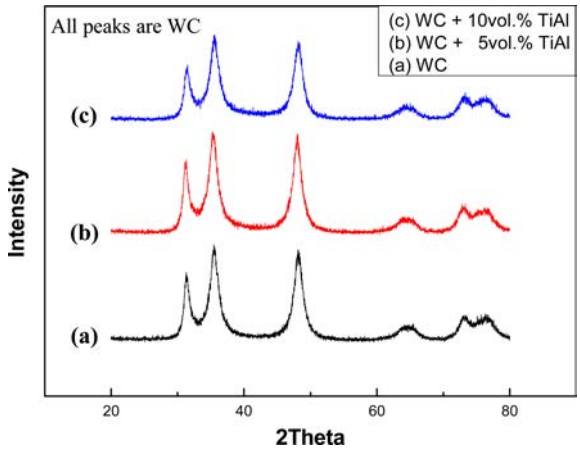

Fig. 4. XRD patterns of (a) WC, (b) WC-5 vol.%TiAl, and (c) WC-10 vol.%TiAl powders milled for 10 h.

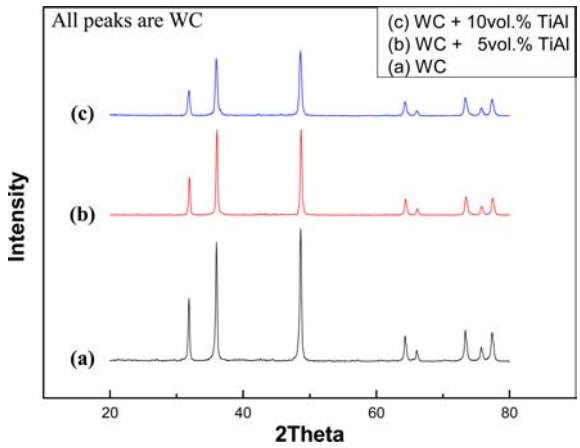

Fig. 5. XRD patterns of (a) WC, (b) WC-5 vol.%TiAl, and (c) WC-10 vol.%TiAl hard materials sintered by PCAS.

are shown in Fig. 6. It is apparent that the WC grains consist of nanocrystallites suggesting the absence of grain growth during sintering. This retention of the fine grain structure can be attributed to the high heating rate and the relatively short exposure to the high temperature. Relative densities corresponding to WC, WC-5 vol.% TiAl, and WC-10 vol.% TiAl were approximately 99, 98.6, and 98.7%, respectively.

The role of the current in sintering has been the focus of several attempts to provide an explanation for the observed sintering enhancement and the improved characteristics of the products. The role played by the current has been variously interpreted. The effect has been explained by fast heating due to Joule heating at contacts points, the presence of plasma in pores separating powder particles, and the intrinsic contribution of the current to fast mass transport [21-25].

Vickers hardness measurements were performed on polished sections of the WC, WC-5 vol.% TiAl, and WC-10 vol.% TiAl samples using a 20 kg load and 15 s dwell time. Indentions with 20 kgf load produced median cracks around the indentation from which fracture toughness can be calculated. The lengths of

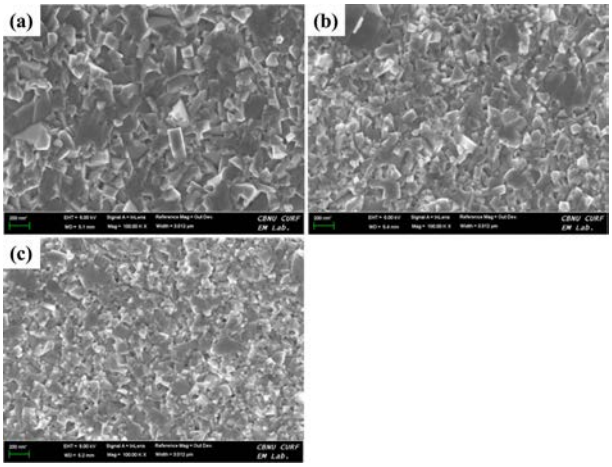

Fig. 6. FE-SEM images of the fracture surface: (a) WC, (b) WC-5 vol.%TiAl, and (c) WC-10 vol.%TiAl hard materials produced by PCAS.

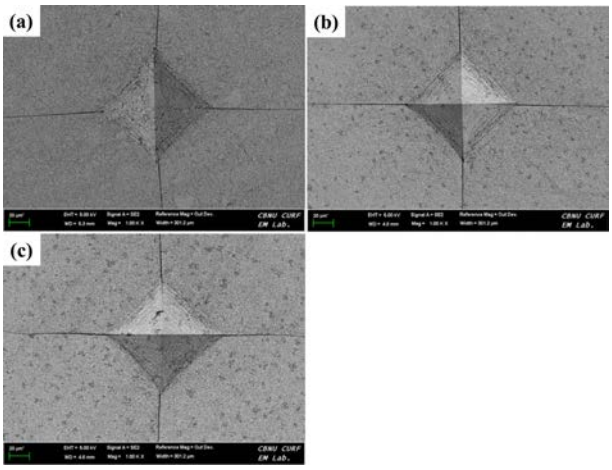

Fig. 7. Vickers hardness indentation in (a) WC (b) WC-5Vol%TiAl (c) WC-10 Vol%TiAl hard materials produced by PCAS.

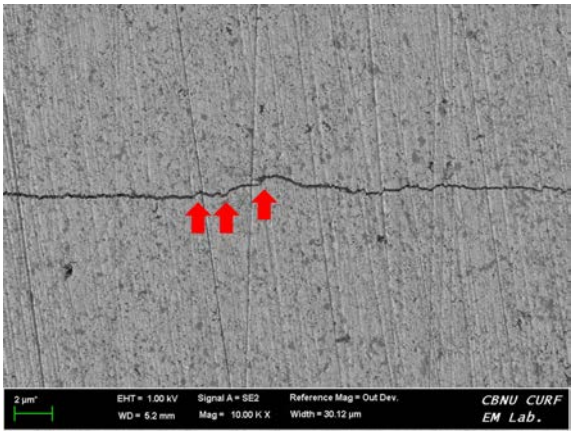

Fig. 8. Crack propagation in WC- 10 Vol%TiAl hard materials produced by PCAS.

these cracks permit estimation of the fracture toughness of the materials by means of the expression [26]:

$$K_{IC} = 0.203(c / a)^{-3/2} \cdot H_v \cdot a^{1/2} \quad (2)$$

where ***c*** is the trace length of the crack measured from the center of the indentation, a is one half of the average length of the two indent diagonals, and H_v is the hardness.

The Vickers hardness and the fracture toughness values of the WC, WC-5 vol.% TiAl, and WC-10 vol.% TiAl samples were 2930 kg/mm^2, 6.5 MPa · m$^{1/2}$, and 2733 kg/mm^2, 8.1 MPa · m$^{1/2}$ and 2576 kg/mm^2, 9 MPa · m$^{1/2}$, respectively. These values represent the average of five measurements. The fracture toughness of WC-5vol.% TiAl, and WC-10 vol.% TiAl samples are higher than that of monolithic WC without great decrease of hardness because the grain size of WC decreases with addition of TiAl. The sintering method in this study was proven to be very effective to consolidate WC-TiAl cermets. The hardness of metal carbide greatly decreased by addition of Co or Ni [28]. The use of TiAl binder instead of Co or Ni is very effective especially to maintain the high hardness of monolithic WC without the expense of toughness reduction. In this regard, it would be worthwhile to consider TiAl as the possible replacement for Co or Ni especially for the applications requiring a high hardness.

Vickers hardness indentations in the WC, WC-5 vol.% TiAl, and WC-10 vol.% TiAl samples show typically one to three additional cracks propagating radially from the indentation as shown in Fig. 7. Fig. 8 shows a crack propagated in a deflective manner (↑) in WC-10 vol.% TiAl composite. The enhanced fracture toughness of WC-10 vol.% TiAl composite is believed that WC and TiAl in the composite may deter the propagation of cracks and WC and TiAl have nanostructure phases.

Conclusions

Using pulsed current activated sintering (PCAS), the rapid consolidation of the WC, WC-5vol.%TiAl, and WC-10 vol.%TiAl was accomplished successfully. Nearly full-dense nanostructured WC and WC-TiAl composites could be obtained within 2 min. The average grain sizes of the WC are about 70, 66, and 50 nm for the samples with WC, WC-5 vol.%TiAl, and WC-10 vol.%TiAl. The Vickers hardness and the fracture toughness values of the WC, WC-5 vol.% TiAl, and WC-10 vol.% TiAl samples were 2930 kg/mm^2, 6.5 MPa · m$^{1/2}$, and 2733 kg/mm^2, 8.1 MPa · m$^{1/2}$ and 2576 kg/mm^2, 9 MPa · m$^{1/2}$, respectively. The addition of TiAl to WC improved the fracture toughness of cemented WC without great reduction of hardness. It would be worthwhile to consider TiAl as the possible replacement for Co or Ni especially for the applications requiring a high hardness.

Acknowledgments

This work was supported by a grant in aid awarded by the Basic Research Project of the Korea Institute of Geoscience and Mineral Resources (KIGAM), funded by the Ministry of Science, ICT and Future Planning

(GP2015036) and this work was supported by the KIST Institutional Program (Project No. 2E25374-15-096).

References

1. H.C. Kim, I.J. Shon, I.K. Jeong, I.Y. Ko, J.K. Yoon, J.M. Doh, Metals and Materials International 13 (2007) 39-45.
2. H. Suzuki, Cemented Carbide and Sintered Hard Materials, Maruzen, Tokyo (1986) 262.
3. S. Imasato, K. Tokumoto, T. Kitada, S. Sakaguchi, Int. J. Refract. Met. Hard Mater. 13 (1995) 305-312.
4. G. Gille, J. Bredthauer, B. Gries, B. Mende, Int. J. Refract. Met. Hard Mater. 18[2-3] (2000) 87-102.
5. H. Lin, B. Tao, J. Xiong, Q. Li, Int. J. Refract. Met. Hard Mater. 41 (2013) 363-365.
6. Z.G. Zhang, F. Gesmundo, P.Y. Hou, Y. Niu, Corrosion Science 48 (2006) 741-765.
7. M. Sherif El-Eskandarany, J. Alloys & Compounds 305 (2000) 225-238.
8. L. Fu, L.H. Cao, Y.S. Fan, Scripta Materialia 44 (2001) 1061-1068.
9. K. Niihara, A. Nikahira, "Advanced structural Inorganic Composite", Elsevier Scientific Publishing Co., Trieste, Italy, 1990.
10. S. Berger, R. Porat, R. Rosen, Progress in Materials 42 (1997) 311-320.
11. I.J. Shon, H.J. Kwon, and H.S. Oh, Electron. Mater. Lett. 10 (2014) 337-343.
12. H.S. Kang, J.M. Doh, J.K. Yoon, and I.J. Shon, Korean J. Met. Mater. 52 (2014) 759-764.
13. F. Charlot, E. Gaffet, B. Zeghmati, F. Bernard, J.C. Liepce, Mater. Sci. Eng. A 262 (1999) 279-278.
14. H.S. Kang and I.J. Shon, Korean J. Met. Mater. 52 (2014) 623-629.
15. M.K. Beyer, H. Clausen-Schaumann, Chem. Rev. 105 (2005) 2921-2948.
16. H.G. Jo and I.J. Shon, Journal of Ceramic Processing Research 15[6] (2014) 371-375.
17. I.J. Shon, Korean J. Met. Mater. 52 (2014) 573-580.
18. B.R. Kang and I.J. Shon, Korean J. Met. Mater. 53 (2015) 255-260.
19. I.J. Shon, H.G. Jo, and H.J. Kwon, Korean J. Met. Mater. 52 (2014) 343-346.
20. Suryanarayana C. and Grant Norton M., "*X-ray Diffraction A Practical Approach*", Plenum Press, New York, 1998.
21. Z. Shen, M. Johnsson, Z. Zhao and M. Nygren, J. Am. Ceram. Soc. 85 (2002) 1921-1927.
22. J.E. Garay, U. Anselmi-Tamburini, Z.A. Munir, S.C. Glade and P. Asoka-Kumar, Appl. Phys. Lett. 85 (2004) 573-575.
23. J.R. Friedman, J.E. Garay, U. Anselmi-Tamburini and Z.A. Munir, Intermetallics. 12 (2004) 589-597.
24. J.E. Garay, U. Anselmi-Tamburini and Z.A. Munir, Acta Mater. 51 (2003) 4487-4495.
25. R. Raj, M. Cologna, and J.S.C. Francis, J. Am. Ceram. Soc. 94[7] (2011) 1941-1965.
26. K. Niihara, R. Morena, and D.P.H. Hasselman, J. Mater. Sci. Lett. 1 (1982) 12-16.
27. I.J. Shon, I.K. Jeong, I.Y. Ko, J.M. Doh, K.D. Woo, Ceramics International 35 (2009) 339-344.